

# Testing the quenching subgrid physics in Green Valley galaxies

Ignacio Ferreras<sup>1,2</sup> , James Angthopo<sup>3,4</sup> and Andrea Negri<sup>1</sup>

<sup>1</sup>Instituto de Astrofísica de Canarias, C/ Vía Láctea s/n, E38205, La Laguna, Tenerife, Spain

<sup>2</sup>Dept. of Physics and Astronomy, University College London, London WC1E 6BT, UK

<sup>3</sup>MSSL, University College London, Holmbury St Mary, Surrey, RH5 6NT, UK

<sup>4</sup>INAF, Osservatorio Astronomico di Brera, Via Brera 28, 20121, Milano, Italy

**Abstract.** In the title of this Symposium: “The rise and fall of star formation in galaxies”, the “falling” stage is mostly represented by so-called Green Valley galaxies. In this phase, quenching mechanisms operate, concerning the evolution from star formation towards quiescence. Therefore, GV galaxies are ideal laboratories to test cosmological simulations. This contribution focuses on the application of a novel, dust-independent, definition of the GV, to two of the most recent simulations: EAGLE and Illustris-TNG. We present some of the results, concerning the excess fraction of quenched galaxies in simulations, with respect to observational data from SDSS. We suggest possible causes for the mismatch.

**Keywords.** galaxies: evolution – galaxies: stellar content – methods: numerical

---

## 1. Introduction

A standard statistical methodology to understand the formation and evolution of galaxies involves the use of bivariate plots where the distribution of various observational measurements are compared. One of the most important of these diagrams is arguably the relation between the mass of a galaxy (in its various guises) and a parameter describing the stellar content: either colour, a more targeted spectral indicator or star formation rate. A bimodality is evident in the distribution, with two major components: the blue cloud (BC) made up of star-forming galaxies, and the red sequence (RS) dominated by passively evolving galaxies (see, e.g., [Strateva et al. 2001](#); [Baldry et al. 2004](#)). In between these two lie the so-called green valley (GV) populated by galaxies that evolve from one group to the other (e.g., [Salim 2014](#)): most often from BC to RS (quenching) but with a second channel from RS to BC (rejuvenation). The GV therefore holds the key to understanding the fundamental processes operating during the evolution of galaxies. Cosmological simulations of galaxy formation are typically calibrated to the scaling relations of general populations of galaxies (see, e.g., [Crain et al. 2015](#)), such as the stellar mass function, the Tully-Fisher relation, or the mass-metallicity relation. While those are the lowest order fundamental constraints, it is important to assess whether this calibration manages to explain more focused phases of evolution. The GV, as a transitioning region where a substantial fraction of the quenching population is found, represents an ideal laboratory to test the details incorporated into the models beyond its resolution (“sub-grid physics”).

[Angthopo et al. \(2019\)](#), as part of the doctoral thesis of the first author, proposed a novel definition of the GV based on the 4000Å break, a spectral indicator that is less affected by systematics concerning dust. Details of this definition on a sample of galaxy

spectra from SDSS are presented in [Angthopo, Ferreras, & Silk \(2020\)](#). This contribution focuses on how GV galaxies can be used to test cosmological models of galaxy formation (based on [Angthopo et al. 2021](#)). We refer interested readers to that paper for details on the material presented here.

## 2. GV galaxies and the quenching of star formation

We make use of the latest galaxy formation models from the EAGLE ([Schaye et al. 2015](#)) and Illustris-TNG ([Nelson et al. 2019](#)) collaborations. We adopt the runs defined inside  $L=100$  Mpc boxes (RefL0100N1504 for EAGLE and TNG100 for Illustris-TNG). We extract the formation histories given by the time evolution of the stellar particles, and combine them with population synthesis models ([Vazdekis et al. 2015](#)) to produce synthetic spectra at the same resolution as SDSS (see [Negri et al. 2022](#), for details). We also homogenise the samples, so that these distributions are equivalent in stellar mass – we match the samples differently in EAGLE and TNG100 as they have different mass distributions. In [Angthopo et al. \(2021\)](#) we show that the  $D_n(4000)$  vs stellar mass diagram is comparable between SDSS and simulations, although the latter produce stronger values of the  $4000\text{\AA}$  break and noticeably flatter trends with stellar mass. The fraction of star-forming, AGN and quiescent galaxies in the GV overall matches the observational constraints. While there is an acceptable level of agreement, we find a discrepancy in the GV concerning the fraction of quiescent galaxies at the massive end. This is the focus of this contribution.

Fig. 1 (left/top) shows the fraction of quenched galaxies in the GV as a function of stellar mass for EAGLE (red, left) and TNG100 (blue, right), as dashed lines. This sample corresponds to the mid-GV (mGV), defined as the mid tercile of the distribution of the  $4000\text{\AA}$  break in GV galaxies, selected in bins of stellar mass. The mGV therefore gives a more focused representation of transitioning galaxies, as it targets the trough of the bimodality between BC and RS. The observational constraint from SDSS is shown as shaded areas. Note the sizeable excess of quenched galaxies at  $\log M_s/M_\odot \gtrsim 10.5$ , especially in TNG100. Such an excess must be related to the way the simulations implement the evolution from star formation to quiescence. In order to look for differences between these two models, Fig. 1 (left/bottom) shows the cumulative stellar mass growth of the galaxies in the two most massive bins, where the discrepancy is largest. Note the difference between both simulations, especially in the most massive bin: while EAGLE assembles the stellar mass from early times in a relatively fast way, followed by rapid quenching at around  $\sim 5$  Gyr, TNG100 builds up the stellar content more gradually, extending to later times, producing the quenching at later cosmological times. Moreover, in this model, once the galaxy is quenched, the system no longer experiences subsequent episodes of star formation – unlike EAGLE, that allows for later phases of star formation within the last  $\sim 1$  Gyr. The TNG100 data could be explained if the quenching subgrid prescriptions need to be strong enough to produce the  $z=0$  results that match the observations. This is clearly a signature of the imposed AGN feedback, given that the biggest discrepancy occurs in the most massive galaxies.

Fig. 1 (right) compares the central black hole mass versus the stellar mass of the galaxy in both simulations, at zero redshift, as labelled. At fixed galaxy mass, TNG100 features systematically higher BH masses. Since the AGN feedback depends on  $M_{\text{BH}}$ , it is expected that TNG100 will inject more energy into the ISM during the AGN phase. Moreover, the prescription for AGN feedback in TNG100 includes a kinetic term that applies to the massive end ( $\gtrsim 10^{10.5} M_\odot$ , [Weinberger et al. 2017](#)). Therefore, TNG100 galaxies in the GV quench at later times and more efficiently. In contrast, a larger fraction of GV galaxies in EAGLE show later episodes of star formation, producing lower quenched fractions that are more consistent with the observational constraints. Independent studies

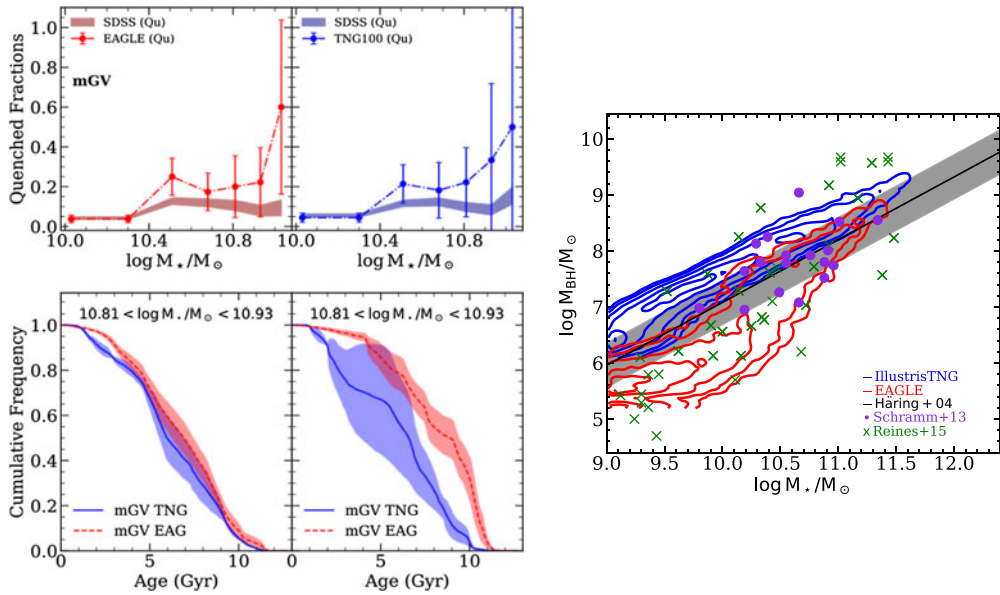


**Figure 1.** *Left:* The top panels show the fraction of quenched GV galaxies as a function of stellar mass for EAGLE (red, left) and TNG100 (blue, right), shown as dashed lines with error bar accounting for the  $1\sigma$  uncertainties. The equivalent observed fraction in SDSS is shown as a shaded region. The sample is defined in the mid tercile of the GV selection. The bottom panels show the cumulative stellar mass growth in the two most massive bins of the sample, for EAGLE (red) and TNG100 (blue). *Right:* The central black hole mass vs stellar mass is shown for EAGLE (red) and TNG100 (blue), with data points from observational constraints. Note the higher black hole mass at fixed stellar mass in the TNG100 simulation. Adapted from Anghopo et al. (2021).

have noted the strong quenching nature of kinetic feedback (see, e.g., Terrazas et al. 2020; Davies et al. 2020), along the lines of our comparisons, but the definition of the sample is important, as other approaches may produce more consistent results with the observations (Donnari et al. 2021). We emphasize that our  $D_n(4000)$ -based definition of the GV provides a robust, dust-independent way of selecting transitioning galaxies. The difference shown in Fig. 1 between the black hole masses of EAGLE and TNG100 galaxies could be down to the systematic difference in seeding the central black holes that eventually act as AGN: Both simulations inject a “seed” BH at the centre, once the dark matter halo reaches a predetermined threshold mass. TNG100 impose a higher BH seed mass, and a higher halo mass threshold (a factor  $\sim 8\times$  higher than EAGLE in both). Along with the kinetic feedback prescription, this choice would statistically induce later AGN-related quenching, which might explain our comparisons with the observational data.

## References

- Anghopo J., Ferreras I., Silk J., 2019, *MNRAS Lett.*, 488, L99  
 Anghopo J., Ferreras I., Silk J., 2020, *MNRAS*, 495, 2720  
 Anghopo J., Negri A., Ferreras I., de la Rosa I. G., Dalla Vecchia C., Pillepich A., 2021, *MNRAS*, 502, 3685  
 Baldry I. K., Glazebrook K., Brinkmann J., Ivezić Ž., Lupton R. H., Nichol R. C., Szalay A. S., 2004, *ApJ*, 600, 681  
 Crain R. A. et al., 2015, *MNRAS*, 450, 1937  
 Davies J. J., Crain R. A., Oppenheimer B. D., Schaye J., 2020, *MNRAS*, 491, 4462

- Donnari M., Pillepich A., Nelson D., Marinacci F., Vogelsberger M., Hernquist L., 2021, *MNRAS*, 506, 4760
- Negri A., Dalla Vecchia C., Aguerri J. A. L., Bahé Y., 2022, *MNRAS*, 515, 2121
- Nelson D., Springel V., Pillepich A., Rodriguez-Gomez V., Torrey P., Genel S., Vogelsberger M., et al., 2019, *Comp. Astronomy & Cosmology*, 6, 2
- Salim S., 2014, *Serb. Astron. J.*, 189, 1
- Schaye J., Crain R. A., Bower R. G., Furlong M., Schaller M., Theuns T., Dalla Vecchia C., et al., 2015, *MNRAS*, 446, 521
- Strateva I., Ivezić Ž., Knapp G. R., Narayanan V. K., Strauss M. A., Gunn J. E., Lupton R. H., et al., 2001, *AJ*, 122, 1861
- Terrazas B. A. et al., 2020, *MNRAS*, 493, 1888
- Vazdekis A., Koleva M., Ricciardelli E., Rčk B., Falcón-Barroso J., 2016, *MNRAS*, 463, 3409
- Weinberger R., Springel V., Hernquist L., Pillepich A., Marinacci F., Pakmor R., Nelson D., et al., 2017, *MNRAS*, 465, 3291